FRAGMENT PRODUCTION FROM THE INTERACTION OF 7.3-BeV π^- *MESONS WITH EMULSION NUCLEI*

Yu. F. GAGARIN and N. S. IVANOVA

A. F. Ioffe Physico-technical Institute, Academy of Sciences, U.S.S.R.

Submitted to JETP editor June 10, 1963

J. Exptl. Theoret. Phys. (U.S.S.R.) 45, 1793-1802 (December, 1963)

Fragment production in interactions between 7.5-BeV π^- mesons and heavy (Ag, Br) emulsion nuclei is investigated. The angle, energy, and charge distributions of the fragments are measured. Disintegrations with and without fragment production are analyzed, and from a comparison with fragmentation induced by pions of different energies it is concluded that cascade nucleons play an important part in the fragmentation process. A comparison of the principal characteristics of the fragments with the corresponding data for hyperfragments leads to some hypotheses regarding hyperfragment formation.

INTRODUCTION

THE investigation of fragment production in interactions between pions and complex nuclei is of special interest because it has been suggested [1] that mesons created in the nuclei play an important part in the fragmentation of nuclei bombarded by high-energy nucleons. Previous investigations [2,3] were concerned with the characteristics of fragment production from heavy emulsion nuclei bombarded with π^+ mesons at relatively low energies (80 and 280 MeV). It was concluded from an analysis of the experimental results that fragment production does not occur in the first stage of interaction between pions and intranuclear nucleons, but is some kind of a secondary process. The data are not inconsistent with the hypothesis that fragmentation is effected by fast nucleons produced in nuclei as a result of pion scattering and absorption.

The fragmentation process is of interest at very high meson energies of the order of several BeV as well as at low energies. The interpretation of the experimental results becomes more difficult at high energies, when multipole meson production plays an important part in individual π-N and N-N interactions within nuclei. However, a study of interactions both with and without fragment production and a comparison of fragmentation characteristics at different incident pion energies yields a definite picture of the effect in which we are interested.

There is an additional reason for being interested in fragmentation caused by very high-energy particles above the threshold of Λ^0 production. A comparison between the principal characteristics of fragments produced under these conditions and the corresponding characteristics of hyperfragments may yield information regarding the production mechanism of the latter.

EXPERIMENTAL PROCEDURE

We used layers of NIKFI-R nuclear emulsion 400 μ thick. A 10 × 20 cm stack was irradiated with a beam of 7.5-BeV π^- mesons (comprising a flux $8 \times 10^3/\text{cm}^2$) from the proton synchrotron of the Joint Institute for Nuclear Research. Our area scanning procedure registered disintegrations, with and without fragments, of heavy emulsion nuclei induced by π^- mesons. Disintegrations observed $\leq 20\,\mu$ from the surfaces of unprocessed emulsion layers were disregarded. Particle tracks were divided into groups according to the customary criteria: thin tracks having grain density $I \leq 1.4\ I_0$ (where the minimum grain density I_0 was that generated by the incident π^- meson), gray tracks having grain density $1.4\ I_0 < I \leq 6.8\ I_0$, and black tracks with grain density $I > 6.8\ I_0$. The disintegration of a heavy emulsion nucleus was assumed if one of the following three conditions was fulfilled: 1) $N_g + N_b$ (the number of gray and black tracks) > 7; 2) the total observable charge associated with gray and black prongs, including the charge of the fragment, was >7; 3) $N_g + N_b < 7$, but the track of a recoil nucleus with range $\leq 3\,\mu$ was observed.

In all cases we measured the angles, projected on the emulsion plane, of thin and gray tracks and of the fragments relative to the incident π^- direc-

tion. The method of Ostroumov and Filov [4] was used to convert the measured angular distributions of particles to space-angle distributions. The charge of a fragment was evaluated by measuring its integral track width as in [2,3].

The determination of the charge was most reliable in the cases of tracks having slopes $\leq 30°$ to the unprocessed emulsion layer. However, in order to augment the statistics we also evaluated the charges of fragments having dip angles from 30° to 60°. The resulting distributions were identical, and our curves were plotted with the data for fragments having dip angles up to 60°. The energies of fragments having determined charges were computed from their ranges in the emulsion. [5]

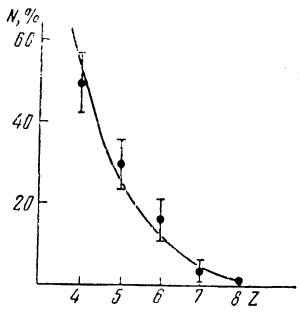

FIG. 1. Charge distribution of fragments with $Z \geq 4$. Experimental points – for incident 7.5-BeV π^- mesons; curve – combined distribution for incident 0.93-, 6.2-, and 9-BeV protons. [6-8]

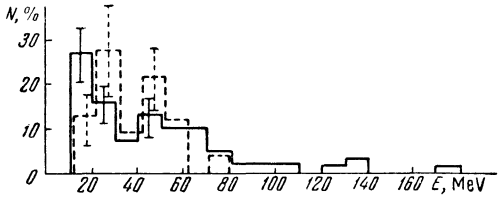

FIG. 2. Energy distribution of fragments with Z = 4 and 5. Continuous histogram – for 7.5-BeV π^- mesons; dashed histogram – for 0.08-BeV π^+ mesons.

EXPERIMENTAL RESULTS

In the present work we analyzed 233 interactions without fragments and 145 interactions with fragments, all of which involved heavy emulsion nuclei; 183 fragments were observed. The following distribution was obtained according to the number of fragments: 78.3% of all stars with fragments contained 1 fragment, 15.9% contained 2 fragments, 4.1% contained 3 fragments, and 0.7% contained 4 fragments.

Cross section. We evaluated the cross section for the production of fragments with $Z \geq 4$ because a considerable number of cases of Z = 3 could have been overlooked during our visual scanning process. In calculating the cross section we took into account the possible omission of registered fragments with angles > 30° to the unprocessed emulsion plane. From our data the cross section for the production of fragments with $Z \geq 4$ from Ag and Br nuclei bombarded with 7.5-BeV π^- mesons is

$$\sigma_{f\ (Z\geqslant 4)} = 70 \pm 15 \text{ mb}.$$

Charge distribution of fragments. The charges of 150 fragments were determined; of these 72 had $Z \geq 4$. Figure 1 shows the fragment charge distribution for $Z \geq 4$. The charge distribution of fragments as given in the literature is represented approximately by a single curve, independently of the kinds and energies of the fragments. [3,6] The same figure shows the combined charge distribution based on several investigations, [6-8] with which our results for 7.5-BeV π^- mesons are in quite good agreement.

Energy distribution of fragments. Figure 2 shows the energy distribution of fragments with Z = 4 and 5 produced by 7.5-BeV π^- mesons (the continuous line). For the purpose of comparison the figure also shows the energy distribution of fragments with the same values of Z in the case of incident 80-MeV mesons (the dashed line). [2] The two energy spectra agree within the experimental error despite the large energy difference of the bombarding pions, as already noted in [3]. Only a small number (~10%) of high-energy fragments were produced in interactions with 7.5-BeV π^- mesons.

Angular distribution of fragments. Figure 3 shows the space-angle distribution of fragments relative to the incident π^- direction (the continuous line). The dashed line represents the angle distribution of gray prongs, which are cascade protons from stars with fragments. The two distributions are very similar.

Characteristics of interactions accompanied by fragment emission. Table I gives the average

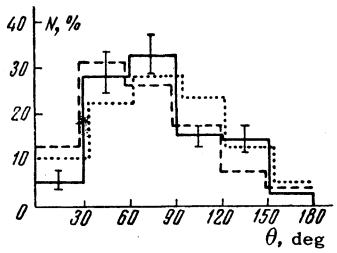

FIG. 3. Space-angle distribution of particles about the direction of the incident 7.5-BeV π^- meson. Continuous histogram – fragments with $Z \geqslant 3$ (experimental); dashed histogram – gray prongs of stars with fragments; dotted histogram – calculated angle distribution of fragments.

Table I

π^- mesons, E = 7.5 BeV	Average No. of Prongs			
	Thin	Gray	Black	Fragments
Interact. producing fragments	3.8±0.3	6.2±0.3	10.3±0.5	1.3
Interact. without fragments	3.3±0.3	4.7±0.3	9.1±0.5	—

numbers of thin, gray, and black prongs in stars with and without fragments. The principal difference between the two distributions is found in the fact that for stars with fragments the average number of gray prons is 31% higher, while the average number of thin prongs is only 17% higher, and that of black prongs is 13% higher.

Figure 4 shows the space-angle distribution of thin prongs about the incident π^- direction. This distribution is considerably broader in stars with fragments. The average emission angle of thin prongs is 45.5 ± 2.4° and 31 ± 2.5° in stars with and without fragments, respectively.

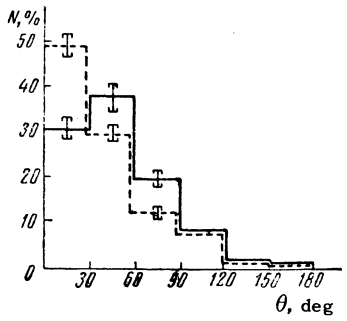

FIG. 4. Space-angle distribution of thin prongs about incident π^- direction. Continuous line – stars with fragments; dashed line – stars without fragments.

DISCUSSION OF RESULTS

Interactions between high-energy particles and complex nuclei have been described by different models. At energies of the order of several BeV the available experimental data do not support a unique choice of the model. Thus, Friedländer regards the "tunnel model" as most probably correct for 9-BeV protons. On the other hand, a Monte-Carlo calculation of the nuclear cascade process in the case of 9-BeV protons was found to be in very good agreement with experiment, so that the authors of [10] prefer the cascade model.

We are able to compare some of our data with calculations [11] on the intranuclear cascade model for interactions of 7.5-BeV π^- mesons with heavy Ag and Br emulsion nuclei. Unfortunately, in [11] the calculated angular distributions of pions and nucleons are given without a division into thin and gray prongs. We have therefore compared the experimental and calculated results for the combined angular distribution of thin and gray prongs. For this purpose 296 interactions with heavy nuclei were measured successively, including 14% with fragments; the results are shown in Fig. 5.

In Fig. 6 we have attempted to compare separately with calculations the angular distributions of thin and gray prongs. The calculated angular distribution of thin prongs is taken to be the distribution of pions accompanied by nucleons with energies > 500 MeV. It was assumed here that all nucleons having energies > 500 MeV are emitted at angles ≤ 30° (lab. system) to the incident π^- directions. Correspondingly, the calculated angular distribution of gray prongs is taken to be the distribution of nucleons after subtracting all those having energies > 500 MeV. The experimental and calculated histograms in Figs. 5 and 6 show good agreement. The calculated average numbers of thin and gray prongs (3.92 and 3.47, respectively) differ somewhat from the experimental results 3.34 ± 0.3 and 4.9 ± 0.3, respectively, for 296 interactions. The calculation neglected meson absorption; this could have reduced somewhat the calculated average number of gray tracks and enhanced the average number of thin tracks. On the

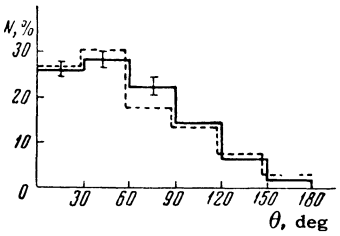

FIG. 5. Combined space-angle distribution of thin and gray prongs about incident π^- direction. Continuous line – experimental; dashed line – calculated.

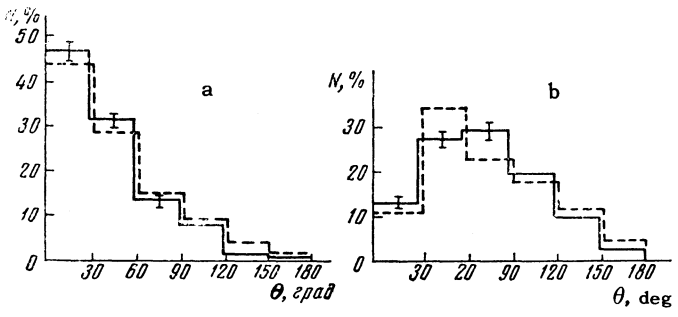

FIG. 6. Space-angle distribution of thin (a) and gray (b) prongs about incident π^- direction. Continuous line – experimental; dashed line – calculated.

Table II

Particle and energy, BeV	Average No. of Prongs			Fragment formation cross section, mb	Excitation energy,[14] MeV	Fragment evaporation probability [14] (Z = 4,5,6)	Fragment forward-to-backward ratio	
	Thin ($\pi^\pm$)	Gray (cascade)	Black (evaporated)				Experimental	Calculated
π^+, E=0.08	0	0.4±0.1	2.6±0.2	1.2±0.5	145	0.010	1.3±0.3	1.05
π^+, E=0.28	0.17±0.06	0.3±0.1	3.9±0.3	1.4±0.5	200	0.031	2.5±0.4	1.14
π^-, E=7.5	3.8±0.13	6.2±0.2	10.3±0.2	70±15	450	0.163	2.2±0.4	1.5
Increase with energy change from 0.08 to 0.28 BeV		1		1		3		
Increase with energy change from 0.28 to 7.5 BeV		20		50		5.3		

other hand, the selection criterion rejected interactions with heavy emulsion nuclei (without recoil nuclei) when $N_g + N_b < 7$. This could have exaggerated the experimental average number of cascade particles.

The foregoing comparisons do not conflict with the intranuclear cascade model for interactions of 7.5-BeV π^- mesons with heavy emulsion nuclei.

We now turn to the characteristics of the fragmentation process. Over a large range of incident meson energy, the principal characteristics of fragments remained practically unchanged (Figs. 1 and 2). From an analysis of interactions with and without fragment emission we conclude that in the case of incident 7.5-BeV mesons the produced fragments are associated mainly with the development of intranuclear nucleon cascades. As already noted, the principal difference in the interactions (Table I) lies in a marked enhancement (31%) of the average number of gray (cascade) particles in the case of stars with fragments, while there are much smaller changes in the average numbers of black (evaporated) and thin (π^- meson) prongs.[1)]

The behavior of the pions (thin prongs) produced in high-energy interactions characterizes to some degree the primary interaction of the incident particles. In our case a small (17%) increase of the average number of thin prongs in disintegrations with fragments is accompanied (Fig. 4) by a broader fragment angle distribution, which evidently indicates a more central interaction of the incident particles. A more highly developed nucleon cascade therefore appears in the nucleus. We also note that the average number of cascade particles increases with the number of fragments in a single disintegration (6 gray prongs in stars with a single fragment and 6 or 8 in stars with two or more fragments), while the angular distribution of fragments about the pion direction coincides approximately with the angular distribution of cascade particles (Fig. 3).

We have calculated the angular distribution of fragments assuming that cascade nucleons are responsible for their formation, taking into account the angular distribution of emerging cascade particles (Fig. 3) and the fragment angle distribution about the cascade nucleons responsible for their formation. The latter distribution was taken from [13] for the case of fragment formation from Ag and Br nuclei by 100-MeV protons;[2)] the calculated angular distribution is represented by the dotted line in Fig. 3. Satisfactory agreement is observed with the experimental distribution (the continuous line).

Additional information concerning the role of cascade particles was obtained by analyzing fragment-producing interactions at different meson energies (0.08, 0.28, and 7.5 BeV). Table II gives the data obtained for disintegrations of heavy nuclei in the emulsion. The second, third, and fourth columns give the average numbers of thin, cascade, and evaporated particles; the fifth column gives the experimental fragmentation cross sections. This table also gives the mean Ag and Br excitation energies calculated from the Le Couteur theory [14] for the average experimental numbers of evaporated particles. The seventh column gives the calculated probabilities of fragment evaporation (with Z = 4, 5, 6) cal-

[1)]At incident energies of several BeV about 95% of the gray prongs represent cascade nucleons and about 85% of the thin prongs represent π mesons. [12]

[2)]It was assumed that all cascade nucleons have energy $\sim$ 100 MeV, representing the mean energy of cascade nucleons. [11]

culated from the same theory for the corresponding excitation energies.

The table shows that the number of cascade particles is practically identical for 0.08- and 0.28-BeV pions. The experimental fragmentation cross section also remains unchanged within error limits. However, the seventh column shows that under the same conditions the probability of fragment evaporation would be multiplied at least three times. With an increase of pion energy from 0.28 to 7.5 BeV the number of cascade particles increases about 20 times, the cross section increases 50 times, and the evaporation probability only 5 times.

The foregoing data show that the increase of the cross section agrees best with the change of the number of cascade particles. The evaporation mechanism apparently makes no important contribution to fragment production. This conclusion is also supported by a comparison of the last two columns.

The eighth column gives the experimental directional asymmetry of the fragments (the forward-to-backward ratios). The ninth column gives the calculated ratios for the case of fragment evaporation from excited nuclei. For π^+ mesons with E = 0.08 and 0.28 BeV we calculated the upper limit of the evaporated fragment asymmetry assuming that the total meson momentum was transferred to the nucleus. For 7.5-BeV π^- mesons the velocity of a nucleus following the evaporation of a fragment was estimated from the experimental asymmetry of black prongs. It appears that the large experimental asymmetry (2.5) of fragment emission in the case of 0.28-BeV pions cannot be accounted for by fragment evaporation, since even if the total meson momentum is transferred to the nucleus the asymmetry of the evaporated fragments is small (only 1.4). It was shown in [3] that the observed asymmetry can be accounted for easily by assigning an important role to recoiling nucleons from the reaction $\pi^+ + N \rightarrow \pi^+ + N$ in fragment production.

In our opinion, therefore, the principal responsibility for fragment production in interactions between high-energy pions and complex nuclei must be ascribed to cascade nucleons resulting from secondary processes as pions interact with intranuclear nucleons. Our data do not favor any one of the possible mechanisms of fragment production involving cascade particles. The process could involve "knocking out" of a substructure from which a nucleon is scattered quasi-elastically [15,3,13] or the knocking out of "binding nucleons" that bind to the nucleus a temporary substructure formed on the nuclear surface.[16]

FRAGMENTS AND HYPERFRAGMENTS

It is interesting to compare the principal characteristics of fragments produced by high-energy particles with the corresponding characteristics of hyperfragments and to analyze the accompanying interactions. For the charge, angle, and energy distributions of hyperfragments we combined the results given in [17-19] for hyperfragments formed under identical conditions, since each individual investigation yielded only a small number.

All the data on hyperfragments used in the present work can be attributed to heavy emulsion nuclei, since the interactions yielding hyperfragments satisfy the criterion $N_g + N_b > 7$. In treating the data we considered only the hyperfragments with ranges $> 20\mu$ in the emulsion; we can regard only these as having been reliably identified.[3)] For fragments with $Z \geq 4$ the charge can be determined reliably only in the cases of ranges $> 25\mu$.

We now present the results obtained from a comparison of the experimental data for fragments and hyperfragments.

1) The charge distribution of hyperfragments agrees very well with that for fragments having $Z \geq 4$. Figure 7 shows data for both hyperfragments and fragments produced by 9-BeV protons. However, for $Z = 3$ there is some discrepancy between the charge distributions. The number of fragments with $Z = 3$ is greater than with $Z = 4$, but no difference is observed in the case of hyperfragments. This discrepancy for small charges

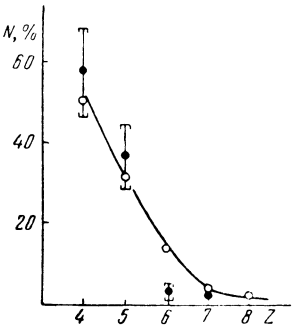

FIG. 7. Charge distributions of fragments and hyperfragments with $Z \geqslant 4$ produced by incident 9-BeV protons. Curve—fragments; black dots—hyperfragments.

[3)] It has been shown in some investigations[20] that the short ranges less than $5-10\mu$ previously atributed to light hyperfragments, may be residual hypernuclei with masses 40–100 amu.

is apparently associated with diminished Λ^0 binding energy for fragments of lower atomic weights. The Λ^0 binding energy becomes comparable to the nucleon binding energy in fragments beginning at about Z = 4.[21]

2. The asymmetry of hyperfragment emission $A_{hf} = N_{hf\,(forward)}/N_{hf\,(backward)}$ agrees with the corresponding result for fragments. For 9-BeV protons we have $A_{hf} = 2.2 \pm 0.2$ [18,19] and $A_f = 2.1 \pm 0.2$.[7]

3. Figure 8 shows the energy distributions of hyperfragments and fragments separately for Z = 3 and Z = 4 or 5 in the case of 9-BeV protons. For fragments these distributions were taken from [22] (for Z = 3) and from [7] (for Z = 4, 5).

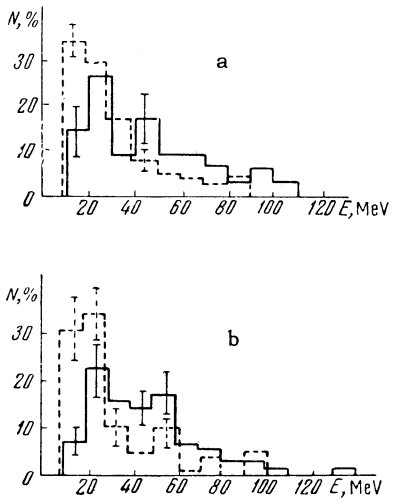

FIG. 8. Energy distributions of fragments and hyperfragments with (a) Z = 3 and (b) Z = 4, 5 produced by 9-BeV protons. Continuous line—hyperfragments; dashed line—fragments (Z = 3 from [22] and Z = 4,5 from [7]).

Within the limits of the relatively small hyperfragment statistics the two histograms agree approximately. It is difficult to determine whether the small difference observed at low energies (10—20 MeV) is significant, since this difference may result from an inaccurate determination of fragment charges in the case of short ranges. In any event, the histograms agree in their general behavior and terminate at about the same energy. The foregoing shows that hyperfragments and fragments have similar characteristics.

A comparison of disintegrations yielding hyperfragments, those yielding fragments, and simple disintegrations reveals a much smaller number (1.6 instead of 3.2) of thin prongs (pions) in the case of hyperfragment formation.[18] This reduced number of emitted pions, if subsequently confirmed, could be accounted for by considering the energy expended in Λ^0 production.[23]

We attempted to evaluate the upper probability limit of hyperfragment production with $Z \geq 4$ from Ag and Br nuclei by 9-BeV protons, using the relative probability of simple fragment production ($Z \geq 4$) from Ag and Br by 9-BeV protons [$\sigma_{f(Z\geq4)}/\sigma_{inel}$] and the relative probability of Λ^0 production [$\sigma_{\Lambda^0}/\sigma_{inel}$] under the same conditions with the nuclear capture ratio K taken into account.[4)] We used the values $\sigma_{inel} = 1000$ mb [10] and $\sigma_{f(Z\geq4)} = 90$ mb [7] for fragment ranges $> 20\mu$. The product $\sigma_{\Lambda^0}K$ was evaluated indirectly from data in [24,25] which yielded $\sigma_{\Lambda^0}K = 2.7 \pm 0.5$ mb. This led to the probability $\rho_{calc} = (\sigma_{\Lambda^0}K/\sigma_{inel})(\sigma_{f(Z\geq4)}/\sigma_{inel}) = (2.4 \pm 1.2) \times 10^{-4}$. The experimental production probability of hyperfragments with ranges $> 20\mu$ and $Z \geq 4$ was taken from [18]: $\rho_{exp} = (1 \pm 0.5) \times 10^{-4}$; our estimate is consistent with this value.

We conclude from the foregoing analysis that the processes of hyperfragment and fragment production are essentially identical, i.e., cascade nucleons are mainly responsible for hyperfragment formation. A Λ^0 particle can exist in a temporary nuclear substructure at the instant of fragment formation or, when the momentum is suitable, the Λ^0 can be captured by an escaping fragment to form a hyperfragment.

We wish to thank S. I. Lyubomilov and the staff of his laboratory for irradiating and processing the emulsion, and Professor N. A. Perfilov for his constant interest in this work.

[1] Wolfgang, Baker, Caretto, Cumming, Friedlander, and Hudis, Phys. Rev. 103, 394 (1956); R. L. Wolfgang and G. Friedlander, Phys. Rev. 96, 190 (1954).

[2] A. S. Assovskaya and N. S. Ivanova, JETP 39, 1511 (1960), Soviet Phys. JETP 12, 1051 (1960).

[3] Ivanova, Ostroumov, and Pavlov, JETP 37, 1604 (1959), Soviet Phys. 10, 1137 (1960).

[4] V. I. Ostroumov and R. A. Filov, PTÉ No. 2, 44 (1957).

[5] A. Papineau, Compt. rend 242, 2933 (1956).

[6] Lozhkin, Perfilov, Rimskiĭ-Korsakov, and Fremlin, JETP 38, 1388 (1960), Soviet Phys. JETP 11, 1001 (1960).

[7] Perfilov, Ivanova, Lozhkin, Makarov, Ostroumov, Solov'eva, and Shamov, JETP 38, 345 (1960), Soviet Phys. JETP 11, 250 (1960).

4) A similar estimate of the probability of hyperfragment production by 2-BeV protons can be found in [24].

[8] Nakagawa, Tamai, and Nomoto, Nuovo cimento 6, 780 (1958).

[9] E. M. Friedländer, Nuovo cimento 14, 796 (1959).

[10] Barashenkov, Maltsev, and Mikhul, Nuclear Phys. 24, 642 (1961); V. S. Barashenkov and V. M. Mal'tsev, Izv. AN SSSR, Ser. Fiz 26, 1069 (1962), Columbia Tech. Transl. p. 1076.

[11] A. Boyadzhiev and V. M. Mal'tsev, Preprint, Joint Inst. Nuclear Res., 1963.

[12] Powell, Fowler, and Perkins, Investigation of Elementary Particles by the Photographic Method, Russ. transl. IIL, 1962, pp. 267, 271.

[13] Arifkhanov, Makarov, Perfilov, and Shamov, JETP 38, 1115 (1960), Soviet Phys. JETP 11, 806 (1960).

[14] Yadernye reaktsii (Nuclear Reactions), Gosatomizdat, 1962, p. 309.

[15] V. I. Ostroumov and R. A. Filov, JETP 37, 643 (1959), Soviet Phys. JETP 10, 459 (1960).

[16] Denisov, Kosareva, and Cerenkov, Materialy konferentsii po mirnomu ispol'zovaniyu atomnoĭ energii (Data of a Conference on the Peaceful Uses of Atomic Energy), Tashkent, 1959.

[17] Tumanyan, Sarinyan, Galstyan, Kanetsyan, Arustamova, and Sarkisyan, JETP 41, 1007 (1961), Soviet Phys. JETP 14, 716 (1962); Arustamova, Kanetsyan, Sarinyan, Toshyan, Tumanyan, and Tumanyan, JETP 44, 861 (1963), Soviet Phys. JETP 17, 581 (1963).

[18] Berkovich, Zhdanov, Lepekhin, and Khokhlova, JETP 41, 75 (1961), Soviet Phys. JETP 14, 57 (1962).

[19] U. G. Gulyamov, Candidate Dissertation, Tashkent, 1961.

[20] Jones, Sanjeevaiah, Zakrzewski, Csejthey-Barth, Lagnaux, Sacton, Beniston, Burhop, and Davis, Phys. Rev. 127, 236 (1962); Zakrzewski, Davis, and Skjeggestad, Nuovo cimento 27, 652 (1963); Nichols, Curtis, and Prowse, Phys. Rev. Letters 1, 327 (1962).

[21] Crayton, Levi Setti, Raymund, Skjeggestad, Abeledo, Ammar, Roberts, and Shipley, Revs. Modern Phys. 34, 186 (1962); Davis, Levi Setti, Raymund, Skjeggestad, Tomasini, Lemonne, Renard, and Sacton, Phys. Rev. Letters 9, 464 (1962).

[22] Bogachev, Grigor'ev, Merekov, and Mitin, JETP 44, 493 (1963), Soviet Phys. JETP 17, 337 (1963).

[23] Berkovich, Zhdanov, Lepekhin, and Khokhlova, JETP 44, 793 (1963), Soviet Phys. JETP 17, 536 (1963).

[24] R. Jastrow, Phys. Rev. 97, 181 (1955).

[25] Belyakov, Glagolev, Kirillova, Mel'nikova, Suk, and Tolstov, Preprint, Joing Inst. Nuclear Research R-434, 1959.

Translated by I. Emin
284